

Accepted Manuscript

Regular paper

Microstrip Broadband Thin-Film Attenuators without Via-hole-ground at Millimeter Wave Frequencies

Beatriz Aja, Eduardo Artal, Enrique Villa, Luisa de la Fuente, Juan Pablo Pascual

PII: S1434-8411(18)31926-5
DOI: <https://doi.org/10.1016/j.aeue.2019.01.005>
Reference: AEUE 52637

To appear in: *International Journal of Electronics and Communications*

Received Date: 17 July 2018
Revised Date: 14 November 2018
Accepted Date: 4 January 2019

Please cite this article as: B. Aja, E. Artal, E. Villa, L. de la Fuente, J. Pablo Pascual, Microstrip Broadband Thin-Film Attenuators without Via-hole-ground at Millimeter Wave Frequencies, *International Journal of Electronics and Communications* (2019), doi: <https://doi.org/10.1016/j.aeue.2019.01.005>

This is a PDF file of an unedited manuscript that has been accepted for publication. As a service to our customers we are providing this early version of the manuscript. The manuscript will undergo copyediting, typesetting, and review of the resulting proof before it is published in its final form. Please note that during the production process errors may be discovered which could affect the content, and all legal disclaimers that apply to the journal pertain.

© 2019. This manuscript version is made available under the CC-BY-NC-ND 4.0 license
<http://creativecommons.org/licenses/by-nc-nd/4.0/>



Microstrip Broadband Thin-Film Attenuators without Via-hole-ground at Millimeter Wave Frequencies

Beatriz Aja^{a,*}, Eduardo Artal^a, Enrique Villa^b, Luisa de la Fuente^a and Juan Pablo Pascual^a

^a Departamento Ingeniería de Comunicaciones, Universidad de Cantabria, Plaza de la Ciencias/n, Santander, 39005, Spain

^b Instituto de Astrofísica de Canarias, IACTec, Via Láctea s/n, 38205 La Laguna, Spain

Abstract

A comprehensive design methodology for microstrip broadband attenuators is presented. Closed-form design equations are given for two types of distributed attenuators. The attenuators are based on a cascade connection of thin-film resistors and microstrip line sections. The structure provides maximally flat attenuation and wideband performance without the need of plated via holes to ground, facilitating manufacture as well as achieving proper performance at millimeter wave frequencies. Experimental results demonstrate the validity of the technique applied to 3 dB and 13 dB broadband attenuators on alumina substrate up to 67 GHz. The proposed topology can be applied not only to MIC, but also to MMIC designs at the highest frequencies.

Keywords: microstrip circuit, MM-wave, thin-film microwave attenuator.

1. Introduction

Attenuators are common passive elements in a wide range of microwave applications with the aim of limiting signal power level or improving the matching between amplification stages, minimizing the gain ripple and adjusting power levels, balancing the power between branches in power dividers, among others [1]-[3]. Conventionally, those attenuators are made of several resistors in Π - or T-topology approaches [4]. At low frequencies, they consist of lumped resistors, while at high ones resistive layer materials are used as thin-film distributed resistors

* Corresponding author: ajab@unican.es (Beatriz Aja)

because of the limitation in the frequency operation of some chip resistors [5]. Several topologies of microwave attenuators have been developed to expand their operation bandwidth, to handle higher power levels, to reduce the size for integration purposes or to achieve significant performances up to high frequencies. Methods of attenuator design have been proposed to widen the frequency band with symmetric U-shaped structures on planar thin-film resistors cascaded through microstrip transmission lines [6] -[9]. On the other hand, different types of resistor fabrication have led to the development of fixed attenuators with different technologies. Π -attenuator topology designs using thin-film embedded resistor technology inserted in grounded coplanar waveguide have been developed up to 40 GHz [10]. Furthermore, the use of semiconductor materials has allowed a size reduction of attenuators and an improved integration with other circuits. It has been demonstrated microstrip attenuators using thin-film cruciform resistors on gallium arsenide (GaAs) substrate from 0 to 40 GHz [11],[12]. On high resistivity silicon substrate up to 20 GHz, attenuators based on tantalum nitride (TaN) thin-film resistor [13]-[15] or with nMOS-switches [16],[17], have been implemented. Moreover, among the microstrip attenuators, the most recent advances are voltage tunable attenuators based on graphene, using microstrip lines connected to ground through graphene pads, which consist of microstrip and lossy transmission lines grounded through via holes [18]-[20]. Although microstrip technologies have been widely used for the realization of microwave attenuators, other technologies have also been used to develop attenuators, such as microwave substrate integrated waveguide (SIW) based on few lossy SIW cavities in shunt connection up to 18 GHz [21] or in combination with surface mount device (SMD) chip resistors in X-band [22]. Most of the described attenuators are fixed and need ground connections, which at millimeter wave frequencies exhibit certain drawbacks. Parasitic effects of plated via holes are quite relevant at these high frequencies and broadband operation cannot be easily achieved. The advantages of

avoiding vias have been outlined for other subcircuits like composite right left hand transmission lines [23]. Other suitable topologies for constant attenuation in very large bandwidths, more than an octave, with connection of thin-film resistors and avoiding via-holes have been demonstrated [13][14], [24]. In this paper, we propose a passive attenuator composed of cascaded thin-film resistors and microstrip line sections. Compared to T- and Π -attenuators, the presented attenuator topology has some advantages as the lack of ground connections. Moreover, closed-form design equations to calculate the attenuator resistors, as a function of the attenuation value, are proposed based on an ideal solution of reference, implemented with lumped resistors. In Section 2, the analytical design and experimental performance of fixed attenuators with two or three resistors and microstrip transmission lines are reported and closed-form design equations are given for these two types of attenuators. Besides, a design methodology for higher attenuation values is described and the case of an eight-resistor attenuator is presented. The dimensions of the attenuators and manufacture details are provided in Section 3. Experimental results of two attenuators, showing good agreement with the simulation, are shown in Section 4. Finally, conclusions are drawn in Section 0.

2. Design of the Attenuators

2.1. Two-resistor attenuator

The simplest attenuator is based on two series resistors separated by a transmission line (Fig. 1). Both resistors, R , have an identical value. The electrical length of the transmission line is $\beta\ell$, and its characteristic impedance is Z_0 .

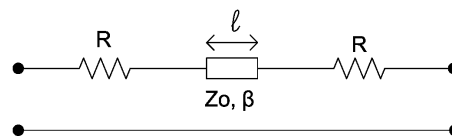
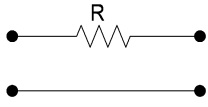
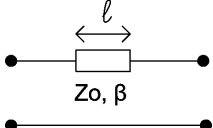


Fig. 1. Schematic diagram of the two-resistor attenuator.

The design method is based on the Scattering parameter analytical equations. They are computed from the ABCD matrix of the attenuator, which can be obtained from the multiplication of the individual ABCD matrixes of the resistors and the transmission line. The ABCD matrix of a series resistor and a transmission line of length ℓ , characteristic impedance Z_0 and phase constant β are given in Table 1.

Table 1 ABCD matrix of series resistor and transmission line

	$\begin{bmatrix} A_R & B_R \\ C_R & D_R \end{bmatrix} = \begin{bmatrix} 1 & R \\ 0 & 1 \end{bmatrix}$		$\begin{bmatrix} A_L & B_L \\ C_L & D_L \end{bmatrix} = \begin{bmatrix} \cos(\beta\ell) & jZ_0 \sin(\beta\ell) \\ jZ_0 \sin(\beta\ell) & \cos(\beta\ell) \end{bmatrix}$
---	---	---	---

The full ABCD matrix of the attenuator can be expressed as

$$\begin{bmatrix} A & B \\ C & D \end{bmatrix} = \begin{bmatrix} A_R & B_R \\ C_R & D_R \end{bmatrix} \begin{bmatrix} A_L & B_L \\ C_L & D_L \end{bmatrix} \begin{bmatrix} A_R & B_R \\ C_R & D_R \end{bmatrix} \quad (1)$$

$$\begin{bmatrix} A & B \\ C & D \end{bmatrix} = \begin{bmatrix} \cos(\varphi) + j\bar{R} \sin(\varphi) & 2R \cos(\varphi) + jZ_0(\bar{R}^2 + 1) \sin(\varphi) \\ jY_0 \sin(\varphi) & \cos(\varphi) + j\bar{R} \sin(\varphi) \end{bmatrix} \quad (2)$$

$$\varphi = \beta\ell \quad (3)$$

where $Y_0 = 1/Z_0$ is the line characteristic admittance, and $\bar{R} = RY_0 = R/Z_0$ is the resistor normalized value. The attenuator is a reciprocal ($S_{21} = S_{12}$) and symmetrical network ($S_{11} = S_{22}$).

Thus, its S-parameters **Error! Reference source not found.** and (5) can be obtained by matrix conversion from the ABCD matrix [4] as follows

$$S_{21} = \frac{1}{(1 + \bar{R}) \cos(\varphi) + j \left(1 + \bar{R} + \frac{\bar{R}^2}{2}\right) \sin(\varphi)} \quad (4) \quad S_{11} = \frac{\bar{R} \cos(\varphi) + j \frac{\bar{R}^2}{2} \sin(\varphi)}{(1 + \bar{R}) \cos(\varphi) + j \left(1 + \bar{R} + \frac{\bar{R}^2}{2}\right) \sin(\varphi)} \quad (5)$$

Finally, the magnitude of S-parameters is given in (6) and (7), as a function of the normalized resistor value and the electrical length.

$$|S_{21}|^2 = \frac{1}{(1 + \bar{R})^2 \cos^2(\varphi) + \left(1 + \bar{R} + \frac{\bar{R}^2}{2}\right)^2 \sin^2(\varphi)} \quad (6)$$

$$|S_{11}|^2 = \frac{\bar{R}^2 \left(\cos^2(\varphi) + \frac{\bar{R}^2}{4} \sin^2(\varphi) \right)}{(1 + \bar{R})^2 \cos^2(\varphi) + \left(1 + \bar{R} + \frac{\bar{R}^2}{2} \right)^2 \sin^2(\varphi)} \quad (7)$$

Insertion loss and matching values are shown in Fig. 2 for four different values of the normalized resistor \bar{R} . Attenuation is mainly determined by the resistor value, while impedance matching is more dependent on the electrical length of the line. The best impedance matching is obtained for low attenuation with low resistor values, while for higher attenuation, higher resistor values produce poor matching results. Thus, this type of attenuators is suitable for low attenuation to have broadband behavior with good matching. The best return loss always occurs for an electrical length of 90° , regardless of the resistor or attenuation values. Therefore, the design rule is very simple: the attenuator design consists of two identical resistors separated by a quarter wavelength line at the center frequency (f_c) of the interest band. At this frequency f_c , (8) and (9) give insertion loss and matching values respectively

$$|S_{21}|^2 = \frac{1}{\left(1 + \bar{R} + \frac{\bar{R}^2}{2} \right)^2} \quad (8) \qquad |S_{11}|^2 = \frac{\bar{R}^4}{4 \left(1 + \bar{R} + \frac{\bar{R}^2}{2} \right)^2} \quad (9)$$

For design purposes, solving (8), the resistor value for a desired attenuation $L = 1/|S_{21}|^2$, is obtained as (10). The best matching achievable, using $\ell = \lambda/4$ at the center frequency, can be calculated as (11).

$$\bar{R} = \sqrt{2\sqrt{L} - 1} - 1 \quad (10) \qquad |S_{11}|^2 = \frac{\left(\sqrt{2\sqrt{L} - 1} - 1 \right)^4}{4} \quad (11)$$

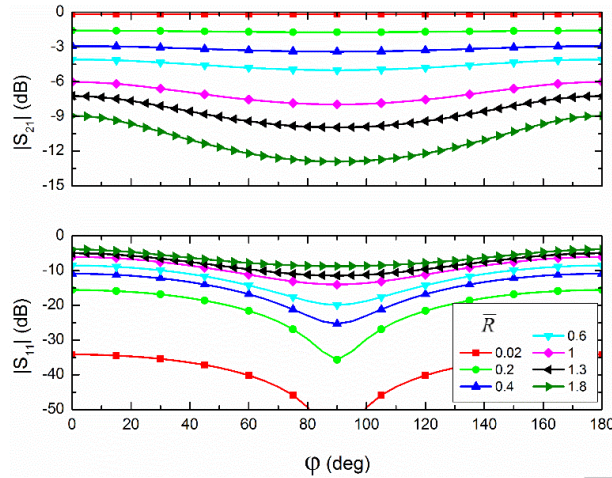


Fig. 2. Insertion loss (S_{21}) and matching (S_{11}) of a two-resistor attenuator versus electrical line length, ϕ , for different resistor values.

Then, from previous expressions, normalized resistor and return loss values can be obtained for several attenuation values, and they are listed in Table 2

Table 2. Attenuation and return loss for two-resistor attenuator

Attenuation L(dB)	Resistor \bar{R}	Return loss (for $\ell=\lambda/4$)
3	0.351	27.21 dB
6	0.729	17.50 dB
10	1.307	11.36 dB
13	1.817	8.65 dB

However, the attenuator based on two-resistor configuration shows unsatisfactory return loss when high attenuation values are desired. Better results are obtained adding a third resistor, as expounded on the next subsection.

2.2. Three-resistor attenuator

A three-resistor attenuator can provide higher attenuation with better impedance matching than a two-resistor attenuator. It has three identical resistors and two transmission lines as depicted in Fig. 3.

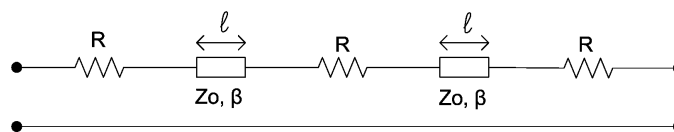


Fig. 3. Schematic diagram of the three-resistor attenuator.

Following the same analysis as in the case of the two-resistor attenuator, the full ABCD matrix can be computed, as defined in (12)

$$\begin{bmatrix} A & B \\ C & D \end{bmatrix} = \begin{bmatrix} \cos(2\varphi) - \bar{R}^2 \sin^2(\varphi) + j\frac{3}{2}\sin(2\varphi) & \bar{R} \left(3\cos^2(\varphi) - (\bar{R}^2 + 2) \sin^2(\varphi) + j \left(\bar{R} + \frac{1}{\bar{R}} \right) \sin(2\varphi) \right) \\ -Y_0(\bar{R} \sin^2(\varphi) + j \sin(2\varphi)) & \bar{R} \left(\cos(2\varphi) - \bar{R}^2 \sin^2(\varphi) + j\frac{3}{2}\sin(2\varphi) \right) \end{bmatrix} \quad (12)$$

By applying matrix conversion, the S-parameters are obtained

$$S_{21} = \frac{2}{-\bar{R}^2 - \frac{\bar{R}^3}{2} + \left(2 + 3\bar{R} + \bar{R}^2 + \frac{\bar{R}^3}{2} \right) \cos(2\varphi) + j(2 + 3\bar{R} + 2\bar{R}^2) \sin(2\varphi)} \quad (13)$$

$$S_{11} = \frac{\bar{R} - \frac{\bar{R}^3}{2} + \left(2\bar{R} + \frac{\bar{R}^3}{2} \right) \cos(2\varphi) + j(2\bar{R}^2) \sin(2\varphi)}{-\bar{R}^2 - \frac{\bar{R}^3}{2} + \left(2 + 3\bar{R} + \bar{R}^2 + \frac{\bar{R}^3}{2} \right) \cos(2\varphi) + j(2 + 3\bar{R} + 2\bar{R}^2) \sin(2\varphi)} \quad (14)$$

and, finally, power magnitudes of S-parameters are obtained from (13) and (14) as

$$|S_{21}|^2 = \frac{4}{\left(-\bar{R}^2 - \frac{\bar{R}^3}{2} + \left(2 + 3\bar{R} + \bar{R}^2 + \frac{\bar{R}^3}{2} \right) \cos(2\varphi) \right)^2 + \left((2 + 3\bar{R} + 2\bar{R}^2) \sin(2\varphi) \right)^2} \quad (15)$$

$$|S_{11}|^2 = \frac{\left(\bar{R} - \frac{\bar{R}^3}{2} + \left(2\bar{R} + \frac{\bar{R}^3}{2} \right) \cos(2\varphi) \right)^2 + \left((2\bar{R}^2) \sin(2\varphi) \right)^2}{\left(-\bar{R}^2 - \frac{\bar{R}^3}{2} + \left(2 + 3\bar{R} + \bar{R}^2 + \frac{\bar{R}^3}{2} \right) \cos(2\varphi) \right)^2 + \left((2 + 3\bar{R} + 2\bar{R}^2) \sin(2\varphi) \right)^2} \quad (16)$$

Using the previous formulation, insertion loss and matching values are assessed and are shown in Fig. 4 for four different \bar{R} resistor values, regarding the same electrical length for both transmission lines. As in the two-resistor attenuator, the attenuation is mainly determined by the resistor value, while the impedance matching also depends on the electrical length of the microstrip lines. When high attenuation is considered, the matching is not outstanding, but it improves for low attenuation values. There are two electrical lengths, around 60° and 120° , which provide the best return losses, regardless of the attenuation value. For high attenuation

values, the optimum electrical length differs from the mentioned values by about 5°. The electrical length values giving the worst return losses are 0°, 90° and 180°.

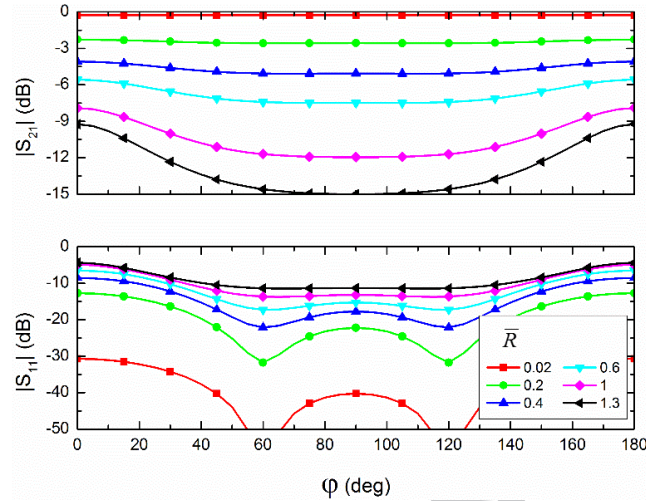


Fig. 4. Insertion loss (S_{21}) and matching (S_{11}) of a three-resistor attenuator versus electrical line length, φ , for different resistor values.

Selecting the shortest electrical length, $\varphi = 60^\circ$, the attenuation is as follows

$$|S_{21}|^2 = \frac{64}{64 + 192\bar{R} + 288\bar{R}^2 + 240\bar{R}^3 + 120\bar{R}^4 + 36\bar{R}^5 + 9\bar{R}^6} \quad (17)$$

For low resistor values, $\bar{R} \ll 1$, the attenuation equation can be simplified. Neglecting third and higher order terms in the denominator of (17), an approximate expression for the resistor value, needed for a desired attenuation L , is as follows

$$\bar{R} \cong \frac{1}{3} \left(\sqrt{L} \left(\sqrt{2 - 1/L} \right) - 1 \right). \quad (18)$$

The error in L (dB) of this design equation increases proportionally to the attenuation, and there is an excess attenuation of almost 3 dB for a nominal value of 10 dB. A more accurate design equation, with an error of 0.64 dB for a 10 dB attenuator, can be obtained maintaining the third order term in the denominator of (17)

$$\bar{R} \cong \frac{1}{5} \left(\sqrt[3]{B_1} - \frac{8}{3\sqrt[3]{B_1}} - 2 \right) \quad (19)$$

where B_1 is given by

$$B_1 = \frac{L}{3} \left(50 - \frac{14}{L} + 10 \sqrt{25 - \frac{14}{L} + \frac{11}{3L^2}} \right) \quad (20)$$

The matching for an electrical length of 60° can be computed by

$$|S_{11}|^2 = \frac{48\bar{R}^4 + 9\bar{R}^6}{64 + 192\bar{R} + 288\bar{R}^2 + 240\bar{R}^3 + 120\bar{R}^4 + 36\bar{R}^5 + 9\bar{R}^6} \quad (21)$$

The performance of the three-resistor attenuator is adequate for attenuation values achievable with $\bar{R} \leq 1$. For higher resistor values, return loss is not acceptable. Besides, the impedance matching degrades for high values of \bar{R} . The best achievable return loss and attenuation versus \bar{R} for a three-resistor attenuator is depicted in Fig. 5. In the case of $\bar{R}=1$, the attenuator S-parameters only depend on the electrical length, so (15) and (16) can be simplified as follows

$$|S_{21}|^2 = \frac{16}{27 \cos^2(2\varphi) + 78 \cos(2\varphi) - 205} \quad (22)$$

$$|S_{11}|^2 = \frac{9 \cos^2(2\varphi) + 10 \cos(2\varphi) + 17}{27 \cos^2(2\varphi) + 78 \cos(2\varphi) - 205} \quad (23)$$

As for the general case of three-resistor attenuators, the electrical length values giving the worst return loss are 0° , 90° and 180° ; while the best return loss can be obtained for lengths of 60° and 120° . The attenuation value for $\bar{R}=1$ is thus 11.84 dB with a maximum return loss value of 12 dB. Therefore, the design of this type of attenuators is feasible, but with three sections, it does not provide good return loss performance for high attenuation values over a wide bandwidth. Their bandwidth is up to one octave, because choosing the minimum frequency to obtain an electrical length of 60° , the double frequency has an electrical length of 120° . Therefore, good return loss and flat attenuation response can be obtained over a broad band. Values of return loss for several attenuation values are shown in Table 3.

Table 3. Attenuation and return loss for three-resistor attenuator

Attenuation L(dB)	Resistor \bar{R}	Return loss ($\varphi=60^\circ$)
3	0.234	29.4 dB
6	0.489	19.6 dB

10	0.896	13.2 dB
13	1.276	10.2 dB

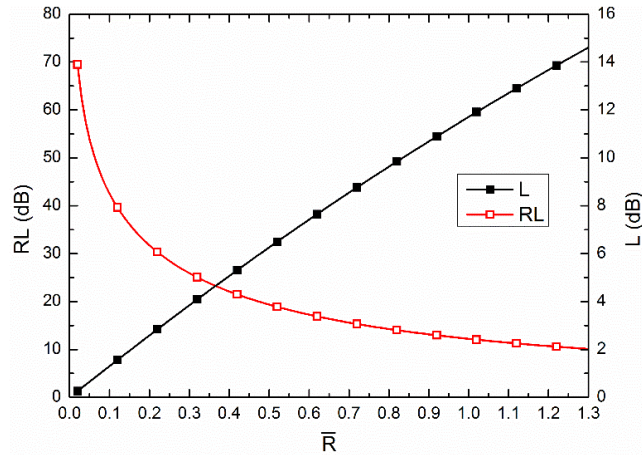


Fig. 5. Best achievable return loss (RL) and attenuation for a three-resistor attenuator versus resistor normalized value \bar{R} .

2.3. Multi-resistor attenuators

Improved impedance matching and higher attenuation values can be obtained adding more resistors and transmission line sections. The condition $\bar{R} \ll 1$ must always be fulfilled to achieve return loss better than 15 dB in at least one octave bandwidth, which implies a high number of sections when high attenuation is required. The attenuation and worst return loss in one octave bandwidth as function of the normalize resistor of attenuators composed of N resistors, with N from 2 to 8 and $\varphi = 90^\circ$ at the central frequency, is depicted in Fig. 6 **Error! Reference source not found.** Normalized resistors lower than 0.5 guarantee return loss better than 15 dB in one octave bandwidth (66.6%) for any attenuator up to 8 sections. For $R \geq 1$ the input impedance of the attenuator tends to have the real part constant and higher than Z_0 , independently of the number of sections. The achievable relative bandwidth with return loss better than 15 dB for attenuators of 3, 6, 10 and 13 dB, composed of different number of sections (N) is depicted in Fig. 7. All the attenuators can provide wide bandwidth with high number of sections, since the normalize resistor has lower value. In addition to bandwidth with good return loss, the attenuation is also flatter for high number of sections, since for a general case of an attenuator

with N resistors, there are $N-1$ line sections and the S_{11} (dB) frequency response has $N-1$ minimum values versus transmission line electrical length (see Fig. 2 and Fig. 4). Therefore, the attenuator design for low attenuation consists of a trade-off between the bandwidth, the nominal value of the resistor, since its tolerance can play a role in its performance, and, maybe less important, the size of the attenuator. On the other hand, high attenuation requires several sections in order to have low normalized resistor and therefore to obtain good return loss over a wide frequency band. Fig. 8 shows the insertion loss and matching versus frequency for N -resistor attenuators for 13 dB attenuation. It is observed that broadband flat attenuation and good return loss are obtained for attenuators with high number of sections.

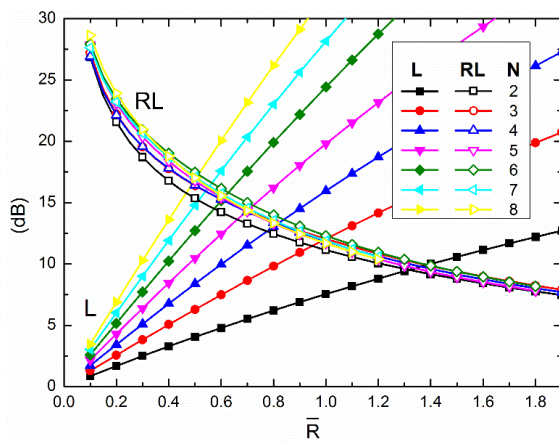


Fig. 6. Attenuation (L) and worst return loss (RL) in one octave bandwidth and for N -resistor attenuator versus resistor normalized value.

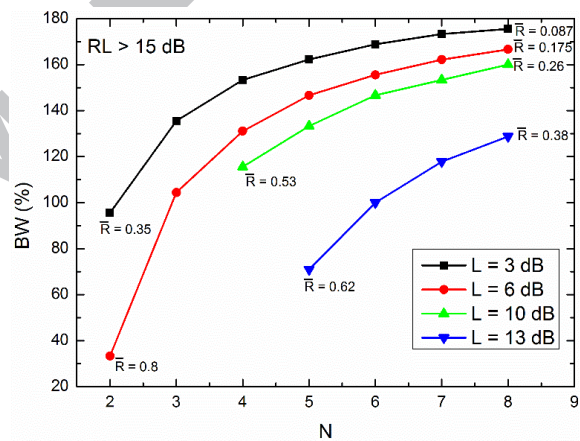


Fig. 7. Relative bandwidth (BW) vs number of sections (N) for return loss better than 15 dB. Normalized resistor value (\bar{R}) is indicated for extreme values of bandwidth.

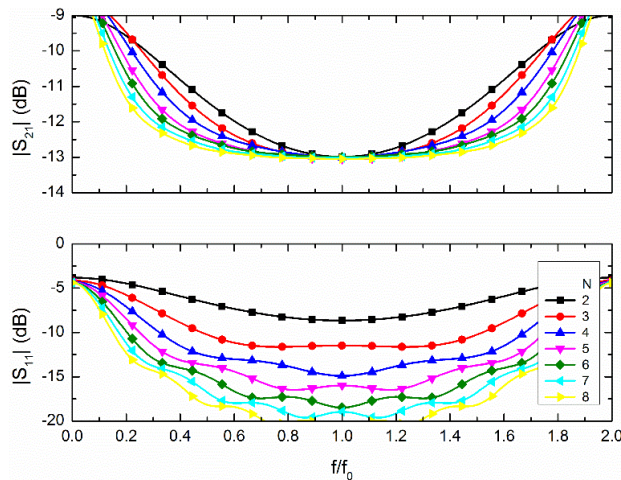


Fig. 8. Insertion loss (S_{21}) and matching (S_{11}) of N-resistor attenuators versus relative frequency for $L = 13$ dB.

A flow diagram to summarize the design procedure is shown in **Fig. 9**. The starting point of the procedure is the attenuator specifications (attenuation L (dB), return loss RL (dB) and bandwidth BW). Initially, $N = 3$ (three resistors) is assumed and the corresponding value of \bar{R} is estimated using (19). Then, MatLab routines compute the Scattering parameters in (13)-(14) with the electrical length φ as a parameter, and the resultant RL and BW are calculated. The fulfillment of RL and BW is verified. If the specified values are not reached, N value is increased in 1 and \bar{R} is recalculated, recomputing the S-parameters using the corresponding equations for the N value and verifying again RL and BW . This loop is repeated until the specifications are fulfilled for a set of values (N, \bar{R}, φ) . Those values together with the initial specifications (L, RL, BW) are the inputs to the attenuator implementation on Advanced Design System (ADS) from Keysight Technologies, for a given technology and substrate properties. After analyzing the proposed topology implemented in the simulator, the design is optimized to compensate, for instance, the electrical length of the resistors to the interconnection transmission lines, providing the best approach to the fulfillment of specifications.

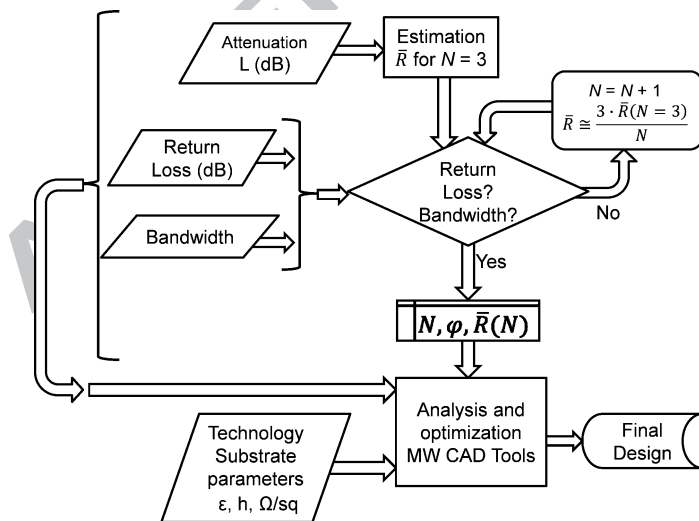


Fig. 9. Flow-diagram of the procedure to attenuator design.

3. Attenuator manufacture

3.1. Microstrip lines and thin-film resistors

Several attenuators have been designed and manufactured for broadband operation centered at 44 GHz, following the design methodology explained in the previous sections. Microstrip lines have been built on Al₂O₃ substrate (alumina), with relative dielectric constant $\epsilon_r = 9.9$, loss tangent $\tan \delta = 10^{-4}$ and thickness $h = 10$ mils. **Table 4** shows details of materials. A thin resistive layer of NiCr providing $20 \Omega/\text{square}$ is deposited over an entire alumina substrate and a gold conductor layer of $3 \mu\text{m}$ thickness is placed on top of that resistive layer. Using a laser process, a transmission line is manufactured removing both layers and leaving the transmission line with the NiCr underneath. Then, using a lithographic process, the resistors are patterned on the transmission line and the gold layer is etched away in the resistors positions. The dimensions of the thin-film resistors can be calculated from the surface resistivity (R_s) of the NiCr resistive layer, the resistor length (ℓ_R) and its width (W), according to (24):

$$R = R_s \frac{\ell_R}{W} \quad (24)$$

To avoid parasitic effects regarding to microstrip step discontinuities, the resistor width, W , was chosen to be the same as the microstrip line width for 50Ω ($W = 260 \mu\text{m}$). Resistor lengths are of the same order of magnitude as microstrip lengths, so their effect must be considered. For example, a 60° line at 44 GHz is $\ell = 419 \mu\text{m}$ physical length, while the 11.68Ω resistor, needed for a 3 dB attenuator, is $\ell_R = 152 \mu\text{m}$. Therefore, microstrip lines between resistors have to be shortened by the resistor length. An optimum value in this example is approximately $\ell = 267 \mu\text{m}$. Two attenuators, shown in Section 4, were designed and manufactured, for nominal attenuations of 3 dB and 13 dB. The first one has three resistors, while the second one has eight resistors.

Table 4. Materials used in attenuator manufacture

Material	Description
Dielectric substrate	Al_2O_3 ($\epsilon_r=9.9$); $h = 10$ mils
Top metal	TiW/Pd + Au ($3 \mu\text{m}$)
Resistive layer	NiCr ($20 \Omega/\text{sq}$)
Resistive layer tolerance	$\pm 20\%$

3.2. Coplanar to microstrip transitions

Coplanar to microstrip transitions were included at input and output attenuator ports. Coplanar lines allow a very accurate experimental characterization using a coplanar probe station for calibration and test. Coplanar line transitions were designed with an electromagnetic (EM) simulator. Both, the coplanar line transitions as well as the complete attenuator have been simulated using the quasi-3D planar EM simulator Momentum, which uses frequency-domain Method of Moments (MoM).

4. Experimental Results

Attenuators with nominal attenuations of 3 dB and 13 dB were tested, and their results were compared with simulations.

4.1. 3 dB attenuator results

A 3-dB thin-film attenuator was fabricated. The data obtained after manufacturing are shown in Table 5. A picture of the attenuator is shown in Fig. 10. Experimental results are shown in Fig. 11.

The measured attenuation was very close to 3 dB over the whole band. For simulation and test comparison, coplanar to microstrip transitions were not considered, because their effect is removed during the test calibration process. In the objective bandwidth of 20 % centered at 44 GHz, return loss was better than 15 dB. The obtained resistor electrical length, ℓ_R , and the transmission line electrical length, ℓ , correspond to phase of $\varphi = 60^\circ$ at 48 GHz

Table 5. Manufacturing data of the 3 dB attenuator

Attenuator	Resistor dimensions	Surface resistivity	Total resistance	Transmission line
------------	---------------------	---------------------	------------------	-------------------

length (mm)	ℓ_R (μm)	W (μm)	(Ohm/sq)	(Ohm)	ℓ (μm)
4.9	142	266	19.8	32	240

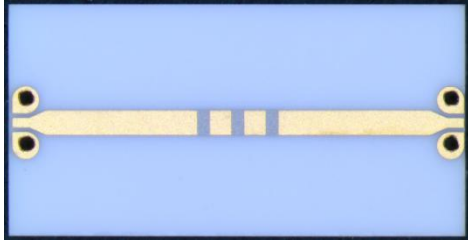


Fig. 10. Manufactured 3-dB attenuator with coplanar to microstrip transitions. Size: 4.9 x 2.5 mm²

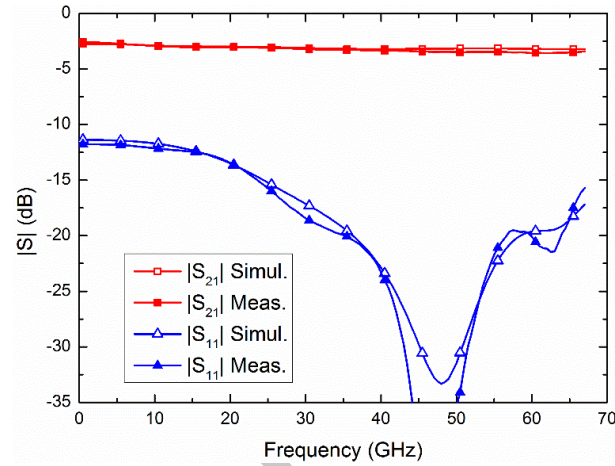


Fig. 11. Test results compared with simulated values or the 3 dB attenuator: input matching $|S_{11}|$ and insertion loss $|S_{21}|$

4.2. 13-dB attenuator results

A 13-dB attenuator was designed and implemented. To achieve the required attenuation, while preserving a good impedance matching, the design was done with eight resistors. Using a thin-film surface resistivity of 20 Ω/sq , the resistor (18.85 Ω) is 245 μm long and 260 μm wide. Microstrip line length between resistors is 350 μm , which accounting for the resistor electrical length is equal to a total electrical length of $\varphi = 90^\circ$ at 44 GHz, with 8 resistors. Manufacturing data are listed in **Table 6**.

Table 6. Manufacturing data of the 13 dB attenuator

Attenuator length (mm)	Resistor dimensions ℓ_R (μm)	W (μm)	Surface resistivity (Ohm/sq)	Total resistance (Ohm)	Transmission line ℓ (μm)
4.9	245	260	20	150	350

A picture of the attenuator is shown in Fig. 12. For testing purposes, it was assembled with commercial coplanar to microstrip line adapters. To compare simulations and tests, the effect of bonding wires, between coplanar to microstrip adapters and attenuator was included, since they are not corrected in the calibration. Three bonding wires with a length of about 150 μm at input and output were used for connection. Experimental results and simulations are shown in Fig. 13.

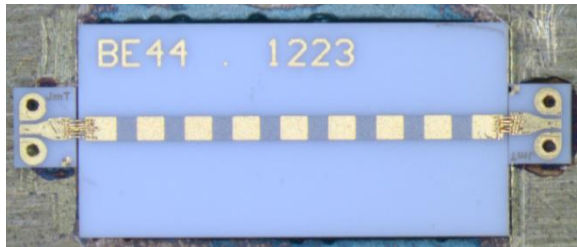


Fig. 12. Manufactured 13-dB attenuator.
Size: 4.9 x 2.5 mm².

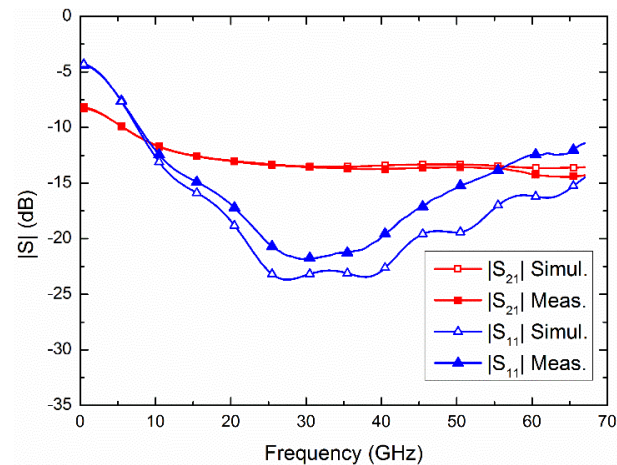


Fig. 13. Test results compared with simulated values for the 13-dB attenuator: input matching $|S_{11}|$ and insertion loss $|S_{21}|$.

The attenuator showed an attenuation of 13 dB in the frequency range of interest. When the bonding wires are included the minimum in $|S_{11}|^2$ is shifted to lower frequencies, since the inductive effect of the bonding wire produces a closer impedance to the center of the Smith chart at around 34 GHz. At low frequencies, the return loss also showed values closer to 10 dB. For both cases, with and without bonding wires, the input matching is good in the required bandwidth.

4.3. Discussion

This section summarizes the results of the presented attenuator design in this manuscript and, at the same time, enables to perform a comparison with described works in the literature. Via-less 3 dB and 13 dB microstrip attenuators with thin-film resistors directly etched over the substrate have been described, performing significant results over a great bandwidth in millimeter-wave frequencies. Table 7 summarizes the comparison of the proposed design with some previously reported works. The moderate sizes of the described circuits are competitive solutions as non-monolithic proposals, as well as, the feasibility of performing quite different attenuation values. Moreover, the flat response over the frequency ensures its use in broadband systems in which equalized gains or responses are required.

Table 7. Comparison with other published State-of-the-Art attenuators

Ref.	Technology	Attenuation Level (dB)	Return Loss (dB)	Operation Bandwidth (GHz)	Physical area (mm ²)
[5]*	Distributed SMD microstrip lines	3, 6, 9, 12	> 7	DC - 40	-
[10]	Thin-film resistors CPWG	6.03	> 17	1 - 32	-
[11]	Thin film resistors in microstrip GaAs MMIC	3, 6, 20	> 23	DC - 40	1 / 2
[12]	Resistive film microstrip lines in GaAs	20	> 23	DC - 40	-
[13]*	Thin film resistors CPW	20	> 27.5	DC - 20	0.448
[14]	Thin-film resistors CPW	10, 15, 20, 30	> 27	DC-25	-
[15]*	MEMS silicon sheet resistance	1, 2, 4, 8	> 22	DC - 20	16.14
[16]*	CMOS	1, 2, 4, 8, 16	> 11	3 - 22	-
[17]*	CMOS	25	> 10	DC - 20	0.098
[20]	Graphene-based microstrip lines	10	-	1 - 20	-
[21]	SIW	12.5	> 16	14.5 – 16.5	-
[22]	SIW	2, 4, 6	> 12	7.6 – 11.6	570
[24]	Thin-film resistors CPW	20, 30	-	1 - 10	61.95
This work	Thin film resistors in microstrip lines	$\frac{3.1}{13}$	> 15	$\frac{25 - 67}{15 - 51}$	12.25

*simulation results

5. Conclusion

Closed-form equations for the design of broadband microstrip thin-film attenuators, with two or three resistors, are presented and a design methodology for a higher number of resistors is proposed. The attenuators are based on a cascade connection of thin-film resistors and microstrip lines, avoiding parasitic effects due to plated via holes to ground in classical T- or Π -type resistive attenuators. Test results for 3-dB and 13-dB broadband attenuators centered at 44 GHz, have experimentally validated the proposed method. The attenuator exhibits high return loss and

maximally flat insertion loss over a wide frequency band. The attenuators presented are very suitable for microwave and millimeter wave frequencies. Furthermore, the size reduction of the presented type of attenuators is also possible using semiconductor materials to design monolithic microwave integrated circuits (MMIC), which allows its integration with other circuits. Moreover, if thin film resistors are replaced by new materials suitable to be biased, like graphene, variable attenuators can be implemented based on the proposed topology.

Acknowledgment

This work was supported by the Spanish Ministry of Economy and Competitiveness mainly under Grant ESP2015-70646-C2-2-R and additionally under Grant TEC2017-83343-C4-1-R, and Ministry of Science, Innovation and Universities under Grant AYA2017-92153-EXP. The authors thank Eva Cuerno for her assistance during the attenuators assembly.

References

- [1] Zhou M, Mo J, Wang Z. A Ka-band low power consumption MMIC core chip for T/R modules. *AEU-Int J Electron Commun* 2018; 91; 37-43.
<https://doi.org/10.1016/j.aeue.2018.04.027>
- [2] Askari M, Kaabi H, Skavian YS. A 24 GHz reflective-type phase shifter with constant loss in 0.18 μm CMOS technology. *AEU-Int J Electron Commun* 2015; 69(8); 1134-42.
<https://doi.org/10.1016/j.aeue.2015.04.015>
- [3] Aja B, Artal E, de la Fuente L, Pascual JP. Effective bandwidth improvement technique based on mismatch analysis. In *Proc. European Microw Conf*, 2006. p.1501-04.
<https://doi.org/10.1109/EUMC.2006.281344>
- [4] Collin RE. *Foundations for Microwave Engineering*. 2nd edition. McGraw-Hill. 1992.

- [5] Otto S, Betray A, Solbach K. A distributed attenuator for K-band using standard SMD thin-film chip resistors. Asia Pacific Microw Conf, 2009; p.2148-51. <https://doi.org/10.1109/APMC.2009.5385509>
- [6] Bogomolov PG. The broadband microwave attenuator. Int Conf Young Specialists Micro/Nanotechnol Electron Devices. 2015. p.110-2. <https://doi.org/10.1109/EDM.2015.7184501>
- [7] Bogomolov PG, Rubanovich MG, Razinkin VP. Methods of expanding the bandwidth of multicascade microwave attenuators. Int Scientific-Tech Conf Actual Problems Electron Instr Eng. 2016. p.54-6. <https://doi.org/10.1109/APEIE.2016.7806366>
- [8] Rubanovich MG, Razinkin VP, Khrustalev VA, Nikolaev GG, Stolyarenko AA, Aubakirov KJ. Broadband microwave attenuators of the high level power. Int Conf Actual Problems Electron Instr Eng. 2014. p.390-2. <https://doi.org/10.1109/APEIE.2014.7040923>
- [9] Rubanovich MG, Razinkin VP, Khrustalev VA, Stolyarenko AA, Bogomolov PG, Vostryakov YV. The microwave attenuator. Int Conf Young Specialists Micro/Nanotechnol Electron Devices. 2017. p.134-7. <https://doi.org/10.1109/EDM.2017.7981727>
- [10] Bauer A, Jakob J, Gmiha R, Hageneder D, Bogner W. Embedded resistors for microwave applications up to 50 GHz on printed circuit boards. In: Proc European Microw Conf, 2013. p.1183-6. <http://doi.org/10.23919/EuMC.2013.668687>
- [11] Zagorodny N, Voronin N, Yunusov IV, Goshin GG, Fateev AV, Popkov AY. Microwave microstrip attenuators for GaAs monolithic integrated circuits. Int Conf Semin Young Specialists Micro/Nanotechnol Electron Devices. 2012. p.67-71. <https://doi.org/10.1109/EDM.2012.6310189>
- [12] Popkov AY, Goshin GG, Fateev AV. Synthesis and optimization of the microstrip attenuator geometric dimensions of the range up to 50 GHz by the equivalent circuit transformation. Int

- Siberian Conf Control Commun. 2013. p. 1-4.
<https://doi.org/10.1109/SIBCON.2013.6693567>
- [13]Zhong Q, Liang X, Liu Z. Design of single thin film resistor network as 20dB attenuator for DC-20GHz application. Int Conf Electron Packag Technol. 2015. p. 297-300.
<https://doi.org/10.1109/ICEPT.2015.7236596>
- [14]Zhong QI, Liu I. Wideband attenuators using distributed resistors for attenuation up to 30 dB. IEICE Electronics Express, 2016;13(10):1-9. <https://doi.org/10.1587/elex.13.20160321>
- [15]Zhong Q, Guo X, Liu Z. A DC-20GHz attenuator design with RF MEMS technologies and distributed attenuation networks. IEEE Int Conf Commun Softw and Netw. 2016. p.352-5.
<https://doi.org/10.1109/ICCSN.2016.7586681>
- [16]Zhang Y, Zhuang Y, Li Z, Ren X, Wang, B, Jing K, Qi Z. A 5-bit lumped 0.18- μm CMOS step attenuator with low insertion loss and low phase distortion in 3–22 GHz applications. Microelectron J. 2014;45(4):468-76. <https://doi.org/10.1016/j.mejo.2014.02.013>
- [17]Askari M, Kaabi H, Kaviani YS. A switched T-attenuator using 0.18 μm CMOS optimized switches for DC-20 GHz. AEU-Int J Electron Commun 2015;69(12):1760-65.
<https://doi.org/10.1016/j.aeue.2015.08.016>
- [18]Bellucci S. Graphene-based tunable microstrip attenuators and patch antenna. Int Semiconductor Conf. 2017. p. 19-2. <https://doi.org/10.1109/SMICND.2017.8101145>
- [19] Yasir M, Bistarelli, Cataldo SA, Bozzi, Perregrini ML, Bellucci S. Enhanced tunable microstrip attenuator based on few layer graphene flakes. IEEE Microw Wireless Compon Lett. 2017;27(4):332-334. <https://doi.org/10.1109/LMWC.2017.2679042>
- [20]Pierantoni L, et al. Broadband Microwave Attenuator Based on Few Layer Graphene Flakes. IEEE Trans Microw Theory Tech 2015;63(8):2491-97.
<https://doi.org/10.1109/TMTT.2015.2441062>

- [21]Liu Z, Zhu L, Xiao. G. A novel microwave attenuator on multilayered substrate integrated waveguide. IEEE Trans Compon Packag Technol 2016;6(7):1106-12. <https://doi.org/10.1109/TCPMT.2016.2572735>
- [22]Eom DS, Lee HY. An X-band substrate integrated waveguide attenuator. Microw. Opt. Technol. Lett. 2014;56(10):2446-49. <https://doi.org/10.1002/mop.28607>
- [23]Nuthakki VR, Dhamodharan S. Via-less CRLH-TL unit cells loaded compact and bandwidth-enhanced metamaterial based antennas. AEU-Int J Electron Commun 2017; 60; 48-58. <https://doi.org/10.1016/j.aeue.2017.06.033>
- [24]Yeh JH, LeFebvre J, Premaratne S, Wellstood FC, Palmer BS. Microwave attenuators for use with quantum devices below 100 mK. J. Appl. Phys. 2017;121: 224501-8. <http://dx.doi.org/10.1063/1.4984894>